Dalton Transactions

PAPER

View Article Online
View Journal | View Issue

Cite this: *Dalton Trans.*, 2014, **43**, 883

Spectroelectrochemical investigation of $Bu_4N[Fe(CO)_3(NO)]$: identification of a reversible EC-mechanism†

Fritz Weisser,[a] Johannes E. M. N. Klein,[b] Biprajit Sarkar*[a] and Bernd Plietker*[b]

Received 23rd July 2013,
Accepted 30th September 2013

DOI: 10.1039/c3dt51998h

www.rsc.org/dalton

$Bu_4N[Fe(CO)_3(NO)]$ displays unique catalytic properties in electron-transfer catalysis such as in allylic substitutions, hydrosilylation, transesterifications, or carbene transfer chemistry. Herein we present a detailed spectroelectrochemical investigation of this complex that unravels an interesting electrochemical–chemical transformation in which two parts of $[Fe(CO)_3(NO)]^-$ are oxidized and undergo a disproportionation in the presence of CO to $[Fe(CO)_5]$ and $[Fe(CO)_2(NO)_2]$. Upon re-reduction the former two complexes regenerate $[Fe(CO)_3(NO)]^-$ to about 85%.

Introduction

The preparation and characterization of iron complexes has been at the center of organometallic research for decades.[1] The fact that this metal plays a central role within the metabolism of living organisms might be regarded as one of the main driving forces.[2] The development or application of defined Fe-complexes in catalysis focused for a long time on oxygenation reactions.[3] Within the past decade the field of Fe-catalysis has witnessed a tremendous comeback and an increasing number of electron-transfer catalyses using defined Fe-complexes have been reported.[4] Considering the fact that the literature is full of structurally defined Fe-complexes one might envision that this field of organometallic catalysis is only in its infancy and has the potential to develop into a key discipline. In order to get there a better understanding of structure–activity relationships and deeper insights into the electrochemical behaviour of the active Fe-complexes are required.[5]

Within the past few years we studied the reactivity of $Bu_4N[Fe(CO)_3(NO)]$ (TBAFe)[6] in various chemical transformations such as allylic substitutions, hydrosilylations, transesterifications, or carbene transfer chemistry. Interestingly this complex displays a high catalytic activity whereas the isoelectronic tetracarbonylferrate[7] is mostly used as a stoichiometric nucleophile in organic synthesis. In order to understand the reasons for the differences in reactivity we performed detailed spectroelectrochemical investigations on $Bu_4N[Fe(CO)_3(NO)]$ and compared them to Amatore's[8] detailed studies on the isoelectronic $(Bu_4N)_2[Fe(CO)_4]$. Herein we report the results of this comparative study.

Results and discussion

The existence of CO and NO as ligands in **1** makes it highly suitable for IR spectroscopic studies because of the easily detectable IR signatures of those and the related ligands.[9] In fact, IR spectroscopic studies and chemical reactivity of $[Fe(CO)_3NO]^-$ have been documented in the literature decades ago.[10] To the best of our knowledge, no reports on the cyclic voltammetry and IR spectroelectrochemical investigations have been reported till now.

The reactivity of $[Fe(CO)_4]^{2-}$, mostly as the di-sodium salt, has been studied in great detail by Collman and co-workers.[7] Due to the immense nucleophilicity the term *supernucleophile* has been associated with $[Fe(CO)_4]^{2-}$.[11] As such, the free anion is usually not observed in solution, but rather a contact ion-pair or a solvent separated ion-pair. It proved therefore challenging to generate the Bu_4N^+ salt, which would undergo deprotonation of the Bu_4N^+ in a Hofmann reaction forming $[HFe(CO)_4]^-$,[8] much like fluoride.[12]

Amatore and co-workers were able to generate this salt *in situ* upon electrochemical reduction of $[Fe(CO)_5]$. Subsequently they could determine the redox potential of the couple $[Fe(CO)_4]^{2-}/[Fe(CO)_4]^-$ in THF–HMPA (95 : 5) without a supporting electrolyte to be −1.95 V.[8]

With this result in mind we turned our attention to the isolectronic complex $[Fe(CO)_3(NO)]^-$. It should be noted that this

[a]*Institut für Chemie und Biochemie, Freie Universität Berlin, Fabeckstraße 34-36, DE-14195 Berlin, Germany*
[b]*Institut für Organische Chemie, Universität Stuttgart, Pfaffenwaldring 55, DE-70569 Stuttgart, Germany. E-mail: bernd.plietker@oc.uni-stuttgart.de*
†Electronic supplementary information (ESI) available. See DOI: 10.1039/c3dt51998h

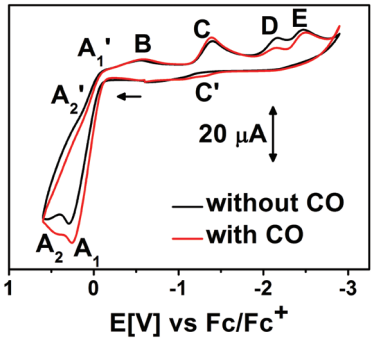

Fig. 1 Cyclic voltammogram of $Bu_4N[Fe(CO)_3NO]$ (**1**) (with and without CO) in THF–0.1 M Bu_4PF_6 measured at 100 mV s^{-1} at 295 K, ferrocene/ferrocenium was used as an internal standard).

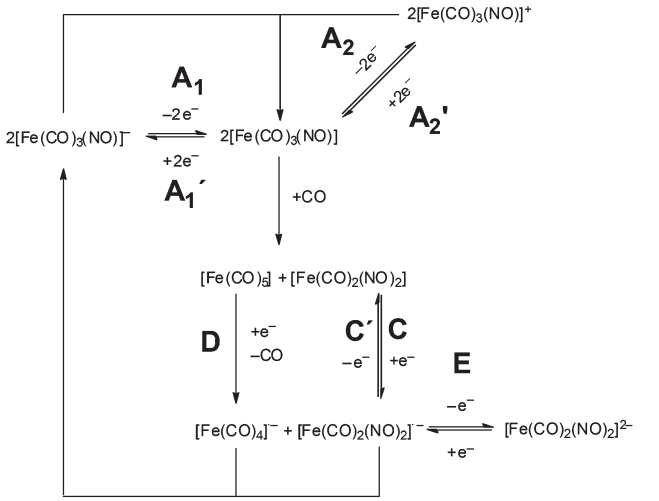

Scheme 1 Mechanism for the cyclic voltammogram (with CO) shown in Fig. 1.

complex can be stored for a prolonged period of time without significant decomposition of its Bu_4N^+ salt. We attribute this stability to the increased π-acceptor properties of the NO-ligand. In addition the choice of the cation, Bu_4N^+, greatly increases stability. As such, we anticipated a well behaved redox-chemistry.

The cyclic voltammogram (CV) of complex $[Fe(CO)_3NO]^-$ exhibits responses which at a first glance look rather complex (Fig. 1). At 295 K in THF–0.1 M Bu_4NPF_6 the CV of $Bu_4N[Fe(CO)_3NO]$ (**1**) shows a main anodic peak at 0.19 V (process A_1) when scanned at a velocity of 100 mV s^{-1} (Fig. 1). On starting at a potential of −0.3 V and scanning the cathodic direction, no responses in the CV are observed if the anodic side is not scanned first. This proves that all cathodic peaks are a follow up of the main anodic peak observed at −0.19 V. The cyclic voltammograms were also recorded in the presence of CO (Fig. 1) and at lower temperatures (Fig. S1†). Those measurements displayed another anodic response at A_2. On reversing the scan direction, cathodic responses are observed at A_1' and A_2' which are re-reduction peaks corresponding to the aforementioned oxidation peaks. Additionally, cathodic responses are observed at −0.52 V (process B), −1.29 V (process C), −2.15 V (process D) and −2.41 V (process E). Furthermore, on reversing the scan direction from negative to positive, a small re-oxidation peak is observed at −1.14 V (process C′). On carrying out the CV measurements in the presence of CO, the peak currents of both A and A′ increased, with A increasing more than A′. The peak current of C increased as well under those conditions, whereas that of D decreased. On carrying out the measurements at 273 K, the absolute peak currents decrease as expected. However, A′ increases compared to A, and the peak currents C, D and E decrease compared to A and A′.

Interpretation of this complex cyclic voltammogram was made easier by the use of literature reports on the chemical reactivity of $[Fe(CO)_3NO]^-$,[10b] and the detection of the intermediates through IR spectroelectrochemistry in the presence and absence of CO. We also have carried out simulations of the cyclic voltammogram to get further insights into the redox mechanism.

Inspired by Amatore's work we propose a mechanism for this complex cyclic voltammetric response which has been validated by IR spectroelectrochemical experiments (Scheme 1). The electron transfer steps shown as "reversible" in Scheme 1 are only meant to imply that small return peaks are observed on reversing the scan direction in those cases. It certainly does not imply electrochemical reversibility as will be discussed below. We first discuss the results obtained in the presence of excess CO.

The complex $[Fe(CO)_3NO]^-$ shows bands for the CO groups at 1983 (A_1), 1877 (E) cm^{-1}, and for the NO at 1647 cm^{-1} (Fig. 2) in THF–0.1 M Bu_4NPF_6. The data matches very well with the literature reports,[10] and confirms the local C_{3v} symmetry of the tetrahedrally coordinated Fe center in $[Fe(CO)_3NO]^-$. The Fe–N–O bond angle has been observed as almost linear in the literature reports of crystallographic data of $[Fe(CO)_3NO]^-$.[13] After processes A_1 and A_2 ($[Fe(CO)_3(NO)]^+$ and $[Fe(CO)_3(NO)]^-$ will comproportionate to $[Fe(CO)_3(NO)]$), in the cyclic voltammogram, the bands corresponding to $[Fe(CO)_3NO]^-$ disappear in its IR spectrum, and these are replaced by new bands at 2088 and 2037 cm^{-1} for ν_{CO} and at 1806 and 1760 cm^{-1} for ν_{NO} which exactly match the IR bands reported for $[Fe(CO)_2(NO)_2]$ (Scheme 1 and Fig. 2).[14] Additionally, there are further bands at 2020 and 1996 cm^{-1} which exactly match the bands reported for $[Fe(CO)_5]$.[15] Thus, electrochemical oxidation of $[Fe(CO)_3NO]^-$ leads to the formation of the unstable species $[Fe(CO)_3NO]$ (Scheme 1) which rapidly decomposes to generate $[Fe(CO)_2(NO)_2]$ and $[Fe(CO)_5]$ as has been unequivocally observed by IR spectroelectrochemistry. Pannell and co-workers have made a related observation earlier while studying the chemical reaction of $[Fe(CO)_3NO]^-$ with CH_3I.[10b] The processes A_1' and A_2' lead to only small changes in the IR spectrum (Scheme 1), the only prominent one being the small regeneration of peaks belonging to $[Fe(CO)_3NO]^-$. Thus, these small peaks are assigned to the re-reduction peak corresponding to A_1 and A_2. The peak B at −0.52 V possibly leads to some decomposition as will be discussed below for measurements in the absence of CO. This peak hardly leads to any changes in the IR spectrum. On reaching peak C, all bands corresponding

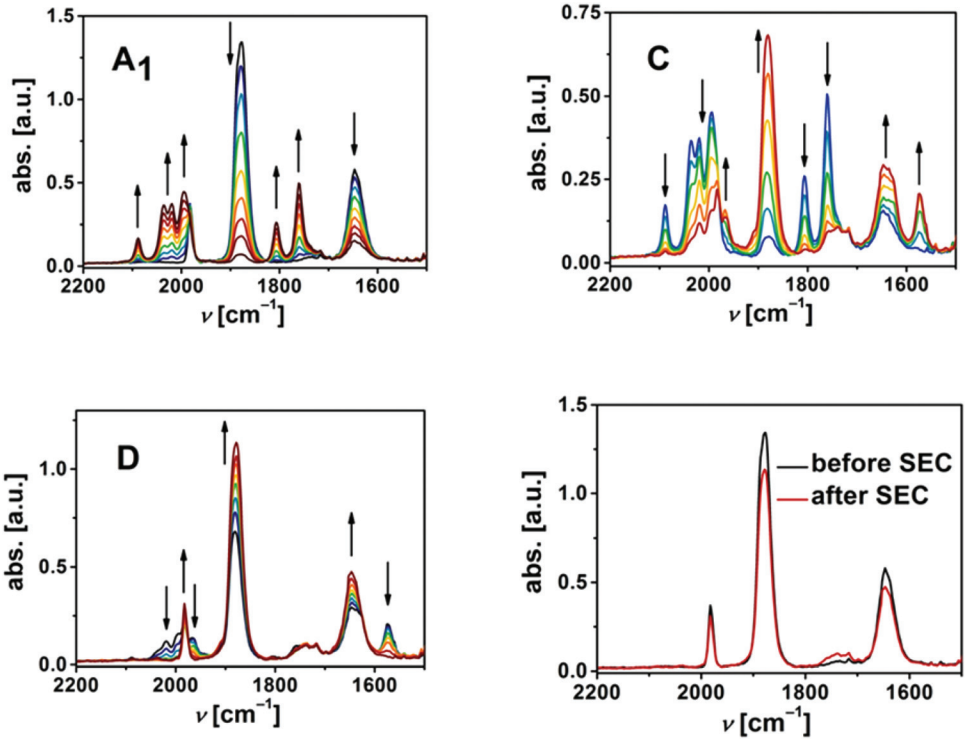

Fig. 2 Changes in the IR spectrum of $Bu_4N[Fe(CO)_3NO]$ (**1**) in the presence of CO during various redox processes (see Scheme 1 for details). Measurements were carried out at 295 K in 0.1 M Bu_4NPF_6–THF.

to $[Fe(CO)_2(NO)_2]$ disappear in the IR spectrum whereas those corresponding to the $[Fe(CO)_5]$ remain intact (Scheme 1 and Fig. 2). Additionally, new bands appear at 1970 and 1882 cm^{-1} for ν_{CO} and at 1625 and 1572 cm^{-1} for ν_{NO}. The potential for process C and the positions of the new bands that appear as a consequence of that process match reasonably well with a recent literature report by Klein *et al.* for the reduction of $[Fe(CO)_2(NO)_2]$ to generate $[Fe(CO)_2(NO)_2]^{\bullet-}$.[14] Hence C represents the reduction by one-electron of $[Fe(CO)_2(NO)_2]$ to generate $[Fe(CO)_2(NO)_2]^{\bullet-}$ (Scheme 1). The potential of −2.15 V for process D matches well with the literature reports for the reduction of $[Fe(CO)_5]$ to generate $[Fe(CO)_5]^{\bullet-}$ (Scheme 2).[15] It is also known from the literature reports that the generated radical anion $[Fe(CO)_5]^{\bullet-}$ is highly unstable, and is capable of reacting with other species in solution or undergoing dimerization.[15] It should be noted that loss of CO is fast and would result in the formation of $[Fe(CO)_4]^{\bullet-}$.[8] In the present case, once process D takes place, the IR bands corresponding to $[Fe(CO)_2(NO)_2]^{\bullet-}$ and $[Fe(CO)_5]$ disappear and these are replaced by new bands at 1983, 1877 and 1647 cm^{-1} which match exactly with the starting substance $[Fe(CO)_3NO]^-$ (Fig. 2). Thus, the reduction of $[Fe(CO)_5]$ to $[Fe(CO)_5]^{\bullet-}$, or possibly $[Fe(CO)_4]^{\bullet-}$, triggers a chemical reaction between this highly unstable anion radical and $[Fe(CO)_2(NO)_2]^{\bullet-}$, leading to the generation of $[Fe(CO)_3NO]^-$ through CO release (Scheme 1).

The peak at −2.41 V (process E) is tentatively assigned to the reduction of $[Fe(CO)_2(NO)_2]^{\bullet-}$ to the dianion $[Fe(CO)_2(NO)_2]^{2-}$ (Scheme 1). This assignment is made based on literature reports on redox potentials for $[Fe(CO)_2(NO)_2]$.[14] The

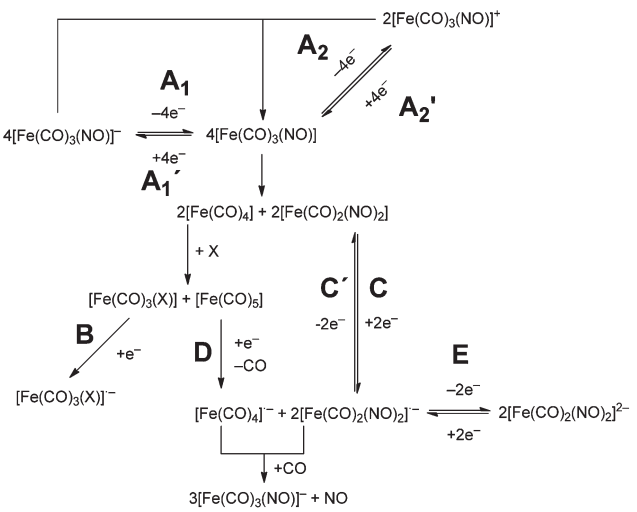

Scheme 2 Mechanism for the cyclic voltammogram (without CO) shown in Fig. 1.

process C′ is assigned to a re-oxidation process (Scheme 1). This process does not lead to any significant changes in the IR spectrum (ESI†). On returning to the starting potential, approximately 85% of the substance is recovered as judged from the intensity of the regenerated IR-bands. These measurements thus deliver a combined electrochemical and chemical transformation which delivers a process that is chemically mostly reversible.

The redox-scheme set up from the IR spectroelectrochemistry measurements also helps in explaining the differences observed in the cyclic voltammograms in the presence and absence of CO, as well as between the measurements carried out at different temperatures. The addition of CO leads to a decrease in the peak current of A_2 because the conversion of $[Fe(CO)_3(NO)]$ to $[Fe(CO)_5]$ and $[Fe(CO)_2(NO)_2]$ is accelerated by CO thus reducing the amount of $[Fe(CO)_3(NO)]$ (Scheme 1). The peak current of C is increased in the presence of CO because CO accelerates the formation of $[Fe(CO)_2(NO)_2]$. Finally, the peak current of D decreases in the presence of CO because reduction of $[Fe(CO)_5]$ is coupled with a loss of CO (Scheme 1). Lowering the temperature of the CV measurements will slow down all the involved chemical reactions, and that in turn will automatically lead to the increase in peak current of A_2 and decrease in those of C, D and E (Scheme 1, Fig. S1†).

When the IR spectroelectrochemistry experiment is performed in the absence of CO gas, there are some important differences. The oxidation process A_1 leads to the same spectral changes, however, the original bands of $[Fe(CO)_3(NO)]^-$ at *ca.* 1875 cm^{-1} and *ca.* 1650 cm^{-1} do not disappear as completely as in the experiments with CO gas (Fig. S2,† top left). Without CO gas the follow-up reaction of $[Fe(CO)_3(NO)]$ is slower, the oxidation of $[Fe(CO)_3(NO)]^-$ to $[Fe(CO)_3(NO)]$ is also slowed down. Due to the slower isomerization, a small amount of $[Fe(CO)_3(NO)]$ is also re-reduced to $[Fe(CO)_3(NO)]^-$ upon reversing the scan direction (Fig. S2,† top right). Reduction C {$[Fe(CO)_2(NO)_2]$ to $[Fe(CO)_2(NO)_2]^-$} proceeds similarly to the experiment with CO gas (Fig. S2,† middle left). However, when $[Fe(CO)_5]$ is reduced (process D), the characteristic band of $[Fe(CO)_2(NO)_2]^-$ at *ca.* 1550 cm^{-1} does not disappear completely (Fig. S2,† middle right). Without CO, a significant amount of $[Fe(CO)_2(NO)_2]^-$ (formed in reduction C) does not recombine with $[Fe(CO)_4]^-$ (formed in reduction D) to the original species $[Fe(CO)_3(NO)]^-$. The leftover $[Fe(CO)_2(NO)_2]^-$ can hence be oxidized back to $[Fe(CO)_2(NO)_2]$ (Fig. S2,† bottom left), which corresponds to process C′. Compared to the IR spectrum measured before the SEC cycle, the bands of $[Fe(CO)_3(NO)]^-$ regain only 70% of their original intensity, and small bands of $[Fe(CO)_2(NO)_2]$ can be seen in the final IR spectrum of the SEC cycle (Fig. S2,† bottom right).

On the basis of these SEC results, we propose a redox scheme for experimental conditions without CO gas (Scheme 2). The IR spectra unambiguously show that $[Fe(CO)_5]$ and $[Fe(CO)_2(NO)_2]$ are formed upon the oxidation of $[Fe(CO)_3(NO)]^-$. The excess CO molecule needed must therefore originate from a complex molecule. We speculate that two molecules of $[Fe(CO)_4]$ react with an additional ligand X, which could be a THF molecule, to form $[Fe(CO)_5]$ and a species $[Fe(CO)_3X]$. As a result, after reduction processes C and D, there are less $[Fe(CO)_4]^-$ molecules than $[Fe(CO)_2(NO)_2]^-$ molecules. This would explain the IR bands of $[Fe(CO)_2(NO)_2]$ at the end of the SEC cycle.

According to the redox scheme (Scheme 2) without CO, we simulated the CV measured with a glassy carbon electrode at 100 mV s^{-1} (Fig. S3†). The simulation features two oxidations A and A′ and a corresponding comproportionation of $[Fe(CO)_3(NO)]^-$ and $[Fe(CO)_3(NO)]^+$ to $[Fe(CO)_3(NO)]$. It also features a fast isomerization of $[Fe(CO)_3(NO)]$ to $[Fe(CO)_2(NO)_2]$ and $[Fe(CO)_4]$ and a slower reaction of $[Fe(CO)_4]$ to $[Fe(CO)_5]$ and $[Fe(CO)_3(X)]$. For the simulation, we assumed that $[Fe(CO)_3(X)]$ is reduced in process B. After the reductions C and D, we simulated a fast recombination of $[Fe(CO)_4]^-$ and $[Fe(CO)_2(NO)_2]^-$ to $[Fe(CO)_3(NO)]^-$. We also assumed that both the species $[Fe(CO)_3(X)]^-$ and $[Fe(CO)_2(NO)_2]^{2-}$ are unstable. Detailed simulation parameters are given in the ESI.†

There are a number of comparisons that can be made to the isoelectronic complex $[Fe(CO)_4]^{2-}$, which has been studied by Amatore and co-workers in a related context (Scheme 3).[8] They investigated both the reduction of $[Fe(CO)_5]$ and the oxidation of $[Fe(CO)_4]^{2-}$ using cyclovoltammetric methods and observed two distinct different mechanisms. At the outcome of these detailed studies they were able to show that $[Fe(CO)_5]$ is reduced under decarbonylation to $[Fe(CO)_4]^-$ and subsequently to $[Fe(CO)_4]^{2-}$, which reacts with $[Fe(CO)_5]$ in a fast reaction to $[Fe_2(CO)_8]^{2-}$ (Scheme 3, right). The same product was observed upon oxidation of $[Fe(CO)_4]^{2-}$ (Scheme 3, left). Whereas the first oxidation step to $[Fe(CO)_4]^-$ is reversible, the dimerization of the latter ferrate to $[Fe_2(CO)_8]^{2-}$ is slow. In both mechanistic scenarios $[Fe_2(CO)_8]^{2-}$ represents the stable endpoint product that is neither being cleaved reductively to give $[Fe(CO)_4]^{2-}$ nor is it being oxidized to give $[Fe(CO)_5]$. The dimerization of $[Fe(CO)_4]^-$ is a very similar process to the reformation of $[Fe(CO)_3NO]^-$ for which an association of $[Fe(CO)_4]^{\bullet-}$ and $[Fe(CO)_2(NO)_2]^{\bullet-}$ followed by ligand exchange and subsequent dissociation to the starting material is likely. Hence, it is the formal exchange of one CO- for one NO-ligand that allows for a "*chemically*" reversible electron transfer in $[Fe(CO)_3(NO)]^-$ and not in $[Fe(CO)_4]^{2-}$. This result clearly indicates the NO-ligand to be the decisive structural motif in electron-transfer catalysis using electron-rich carbonyl ferrates. Moreover, with regard to the results presented above a disproportionation of $[Fe(CO)_4]^-$ into $[Fe(CO)_5]$ and $[Fe(CO)_4]^{2-}$ similar to the reaction of $[Fe(CO)_3(NO)]$ into $[Fe(CO)_5]$ and $[Fe(CO)_2(NO)_2]$ cannot be excluded. This disproportionation reaction could connect the two mechanistic scenarios observed by Amatore and coworkers.

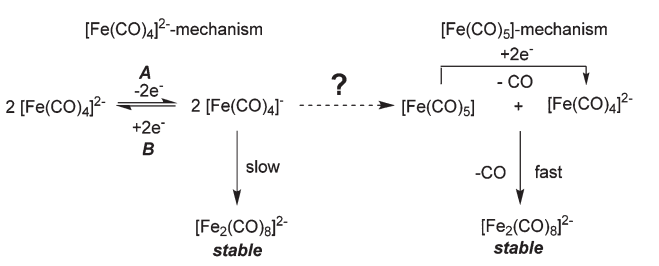

Scheme 3 Redox-chemistry of $[Fe(CO)_5]$ and $[Fe(CO)_4]^{2-}$.[8]

Conclusion

As the anion $[Fe(CO)_3(NO)]^-$ (**1**) is isoelectronic to $[Fe(CO)_4]^{2-}$, the Collman reagent,[7] its electrochemistry has been studied in a related context. Indeed, partial decomposition was observed resulting in $[Fe(CO)_5]$ and $[Fe(CO)_2(NO)_2]$. The defined Fe-carbonyl complexes undergo a single-electron reduction to the corresponding dianions which dimerize and are cleaved to regenerate the respective $[Fe(CO)_3(NO)]^-$ in about 80% yield. The chemically reversible mechanism presented here is in strong contrast to the non-reversible ECE-mechanism observed in cyclovoltammetric studies on the isoelectronic $[Fe(CO)_4]^{2-}$ and underline the importance of the NO-ligand for maintaining catalytic activity.

Notes and references

1 *Comprehensive Organometallic Chemistry II*, ed. D. F. Schriver and M. I. Bruice, Pergamon Press, 2002.
2 (*a*) J. L. Beard, H. Dawson and D. J. Pinero, *Nutr. Rev.*, 1996, **54**, 295–317; (*b*) P. Aisen, C. Enns and M. Wessling-Resnick, *Int. J. Biochem. Cell Biol.*, 2001, **33**, 940–959; (*c*) A. D. Sheftel, A. B. Mason and P. Ponka, *Biochim. Biophys. Acta*, 2012, **1820**, 161–187; (*d*) L. Tandara and I. Salamunic, *Biochem. Med.*, 2012, **22**, 311–328.
3 For representative reviews see: (*a*) L. Que Jr. and R. Y. N. Ho, *Chem. Rev.*, 1996, **96**, 2607–2624; (*b*) M. Costas, M. P. Mehn, M. P. Jensen and L. Que Jr., *Chem. Rev.*, 2004, **104**, 939–986.
4 For selected reviews on iron catalysis see: (*a*) *Iron Catalysis: Fundamentals and Applications: 33 (Topics in Organometallic Chemistry)*, ed. B. Plietker, Springer, Berlin, 2010, vol. 1; (*b*) *Iron Catalysis in Organic Chemistry: Reactions and Applications*, ed. B. Plietker, Wiley-VCH, Weinheim, 2008, vol. 1; (*c*) C. Bolm, J. Legros, J. Le Paih and L. Zani, *Chem. Rev.*, 2004, **104**, 6217–6254; (*d*) A. Correa, O. García Mancheño and C. Bolm, *Chem. Soc. Rev.*, 2008, **37**, 1108–1117; (*e*) W. M. Czaplik, M. Mayer, J. Cvengroš and A. Jacobi von Wangelin, *ChemSusChem*, 2009, **2**, 396–417; (*f*) R. H. Morris, *Chem. Soc. Rev.*, 2009, **38**, 2282–2291; (*g*) L. Liang-Xian, *Curr. Org. Chem.*, 2010, **14**, 1099–1126; (*h*) M. Darwish and M. Wills, *Catal. Sci. Technol.*, 2012, **2**, 243–255; (*i*) K. Gopalaiah, *Chem. Rev.*, 2013, **113**, 3248–3296; (*j*) B. D. Sherry and A. Fürstner, *Acc. Chem. Res.*, 2008, **41**, 1500–1511; (*k*) J. E. M. N. Klein and B. Plietker, *Org. Biomol. Chem.*, 2013, **11**, 1271–1279.
5 R. G. Compton and C. E. Banks, *Understanding Voltammetry*, World Scientific Pub. Co. Pte. Ltd., Singapore, 2007.
6 (*a*) B. Plietker and A. Dieskau, *Eur. J. Org. Chem.*, 2009, 775–787; (*b*) B. Plietker, *Synlett*, 2010, 2049–2058; (*c*) J. E. M. N. Klein, *Synlett*, 2011, 2757–2758.
7 J. P. Collman, *Acc. Chem. Res.*, 1975, **8**, 342–347.
8 (*a*) C. Amatore, J.-N. Verpeaux and P. J. Krusic, *Organometallics*, 1988, **7**, 2426–2428; (*b*) C. Amatore, P. J. Krusic, S. U. Pedersen and J.-N. Verpeaux, *Organometallics*, 1995, **14**, 640–649.
9 (*a*) A. K. Das, B. Sarkar, C. Duboc, S. Strobel, J. Fiedler, S. Zalis, G. K. Lahiri and W. Kaim, *Angew. Chem., Int. Ed.*, 2009, **48**, 4242–4245; (*b*) A. Paretzki, H. S. Das, F. Weisser, T. Scherer, D. Bubrin, J. Fiedler, J. E. Nycx and B. Sarkar, *Eur. J. Inorg. Chem.*, 2011, 2413–2421; (*c*) J. Pellegrino, R. Hübner, F. Doctorovich and W. Kaim, *Chem.–Eur. J.*, 2011, **17**, 7868–7874; (*d*) S. Berger, A. Klein, W. Kaim and J. Fiedler, *Inorg. Chem.*, 1998, **37**, 5664–5671.
10 (*a*) W. Hieber and H. Beutner, *Z. Naturforsch., Teil B*, 1960, **15**, 323–324; (*b*) K. H. Pannell, Y.-S. Chen, K. Belknap, C. C. Wu, I. Bernal, M. W. Creswick and H. N. Huang, *Inorg. Chem.*, 1983, **22**, 418–427; (*c*) W. Hieber and H. Beutner, *Z. Anorg. Allg. Chem.*, 1963, **320**, 101–111.
11 J. P. Collman, R. G. Finke, J. N. Cawse and J. I. Brauman, *J. Am. Chem. Soc.*, 1977, **99**, 2515–2526.
12 H. Sun and S. G. DiMagno, *J. Am. Chem. Soc.*, 2005, **127**, 2050–2051.
13 L. M. Clarkson, W. Clegg, D. C. R. Hockless and N. C. Norman, *Acta Crystallogr., Sect. C: Cryst. Struct. Commun.*, 1992, **48**, 236–239.
14 A. Klein, Y. von Mering, A. Uthe, K. Butsch, D. Schaniel, N. Mockus and T. Woike, *Polyhedron*, 2010, **29**, 2553–2559.
15 D. J. Curran, P. B. Graham and M. D. Rausch, *Organometallics*, 1993, **12**, 2380–2382.